

Electronic Supplementary Information

Article

Vanadium Complexes with Methyl-substituted 8-Hydroxyquinolines: Catalytic Potential in the Oxidation of Hydrocarbons and Alcohols with Peroxides and Biological Activity

Joanna Palion-Gazda¹, André Luz^{2,3}, Luis R. Raposo^{2,3}, Katarzyna Choroba¹, Jacek E. Nycz¹, Alina Bieńko⁴, Agnieszka Lewińska⁴, Karol Erfurt⁵, Pedro V. Baptista^{2,3}, Barbara Machura^{1,*}, Alexandra R. Fernandes^{2,3*}, Lidia S. Shulpina⁶, Nikolay S. Ikonnikov⁶, Georgiy B. Shul'pin^{7,8,*}

¹Institute of Chemistry, University of Silesia, Szkolna 9, 40-006 Katowice, Poland. Email: barbara.machura@us.edu.pl

²Associate Laboratory i4HB - Institute for Health and Bioeconomy, NOVA School of Science and Technology, NOVA University Lisbon, 2819-516 Caparica, Portugal. Email: ma.fernandes@fct.unl.pt

³UCIBIO – Applied Molecular Biosciences Unit, Department of Life Sciences, NOVA School of Science and Technology, NOVA University Lisbon, 2819-516 Caparica, Portugal

⁴Faculty of Chemistry, University of Wroclaw, F. Joliot-Curie 14, 50-383 Wroclaw, Poland

⁵Department of Chemical Organic Technology and Petrochemistry, Silesian University of Technology, Krzywoustego 4, 44-100 Gliwice, Poland

⁶A.N. Nesmeyanov Institute of Organoelement Compounds, Russian Academy of Sciences, ulitsa Vavilova 28, Moscow 119991, Russia, e-mail: shulpina@ineos.ac.ru

⁷N.N. Semenov Federal Research Center for Chemical Physics, Russian Academy of Sciences, ulitsa Kosygina 4, Moscow 119991, Russia, e-mail: gbs@mail.ru

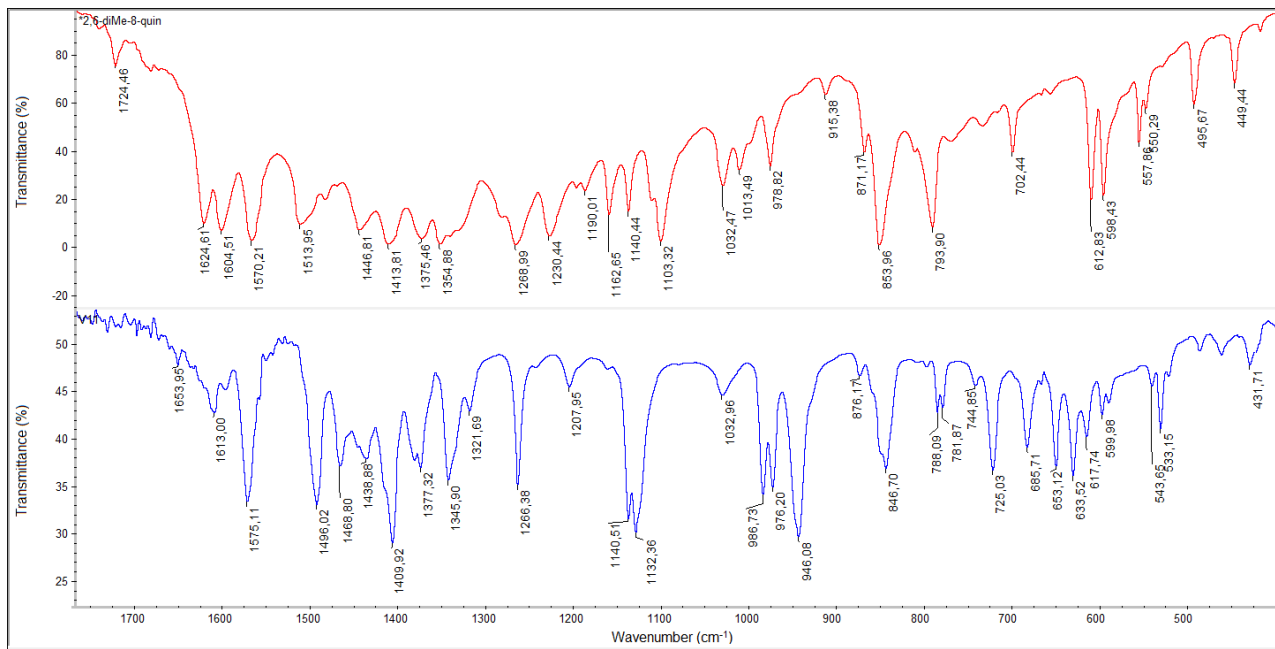
⁸Chair of Chemistry and Physics, Plekhanov Russian University of Economics, Stremskiy pereulok 36, Moscow 117997, Russia

*Correspondence: barbara.machura@us.edu.pl, ma.fernandes@fct.unl.pt; gbs@mail.ru

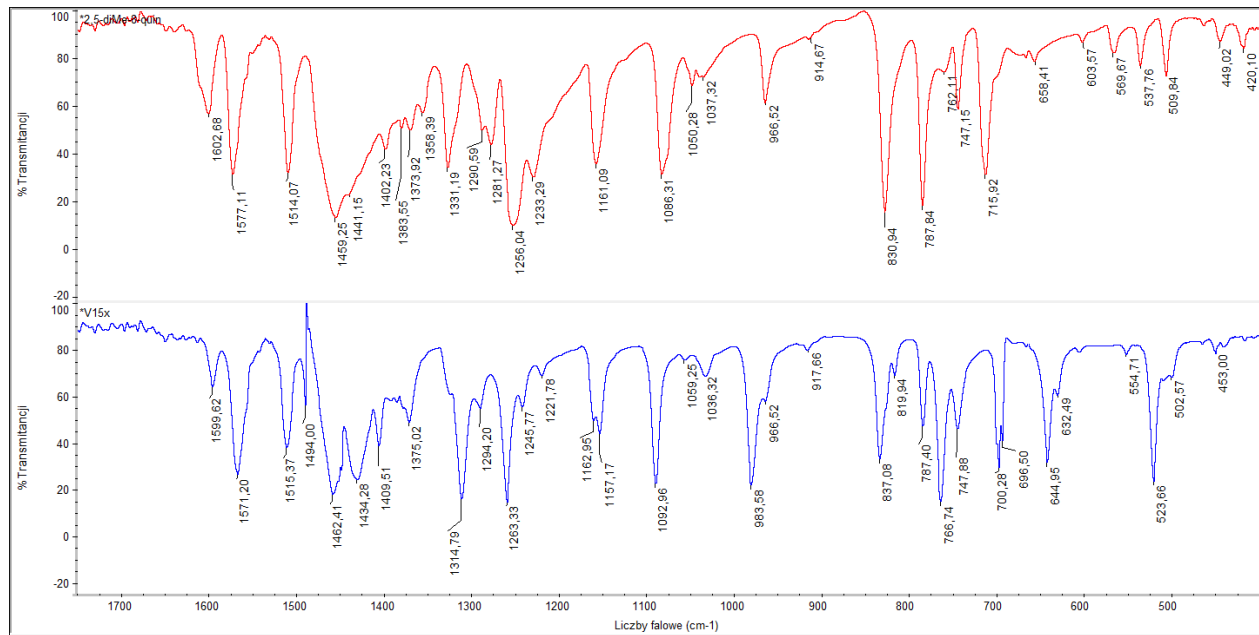
Table of Contents

<i>General Characterization</i>	
IR spectra of complexes 1–3 and free ligands	Figure S1
HRMS of complexes 1–3	Figure S2
<i>X-ray studies</i>	
Selected bond lengths and angles for 1–3	Table S1-S3
Short intra- and intermolecular hydrogen bonds.	Table S4
Short $\pi \cdots \pi$ interactions.	Table S5
X–Y \cdots Cg(J)(π -ring) interactions.	Table S6
Hirshfeld surface and 2D fingerprint plot for 1–3 , together with the relative contributions of various intermolecular interactions to the Hirshfeld surface	Figure S3-S5
View of the intermolecular interactions and packing in 1–3 .	Figure S6-S8
The selected structural parameters of five-coordinated vanadium(IV) complexes	Table S7
X-ray powder diffraction patterns of 3	Figure S9
<i>EPR spectra</i>	
EPR frozen solution spectra (at 77 K) of compounds 1–3 ; in acetonitrile	Figure S10
<i>Absorption spectroscopy</i>	
UV-Vis spectra of complexes 1–3	Figure S11
UV-Vis stability spectra in DMSO of 1–3	Figure S12
<i>Catalytic data</i>	
Oxidation of cyclohexane catalyzed by oxido-V/PCA/aq.H ₂ O ₂ /CH ₃ CN systems	Table S8
<i>Biological results</i>	
Antiproliferative effect of complexes 1–3 in normal dermal fibroblasts, after 48 h. evaluated by the MTS method.	Figure S13
Cell viability of HCT116 cells.	Figure S14

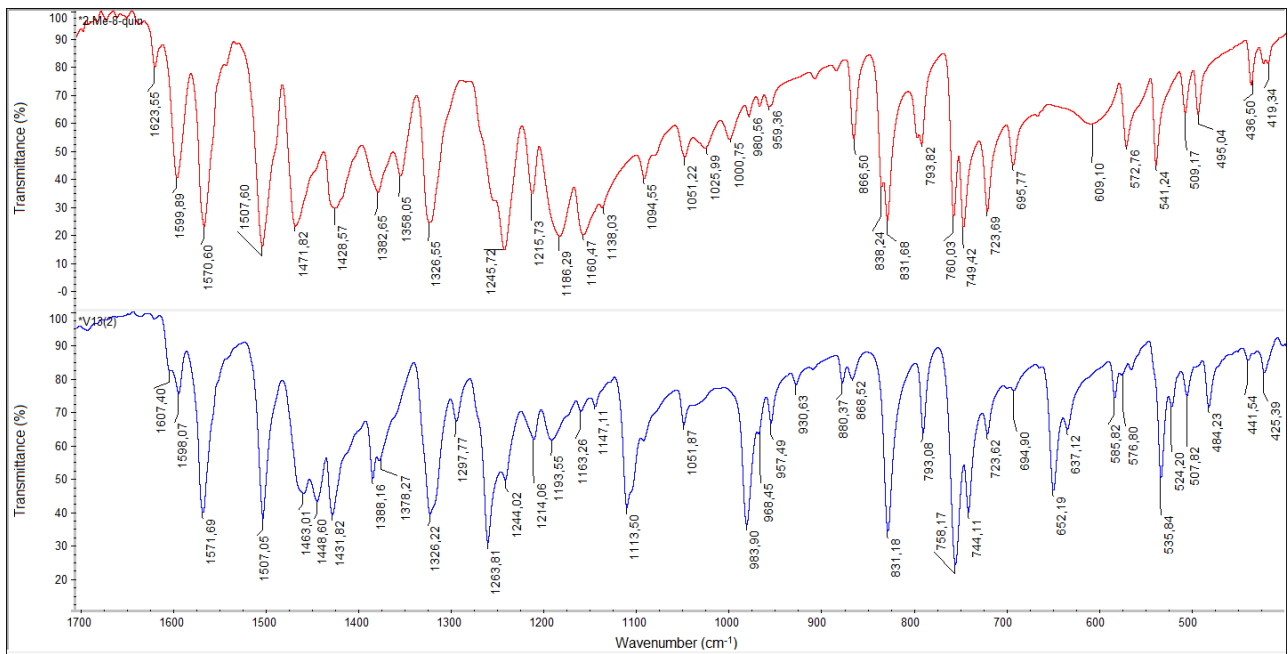
General Characterization



(a)

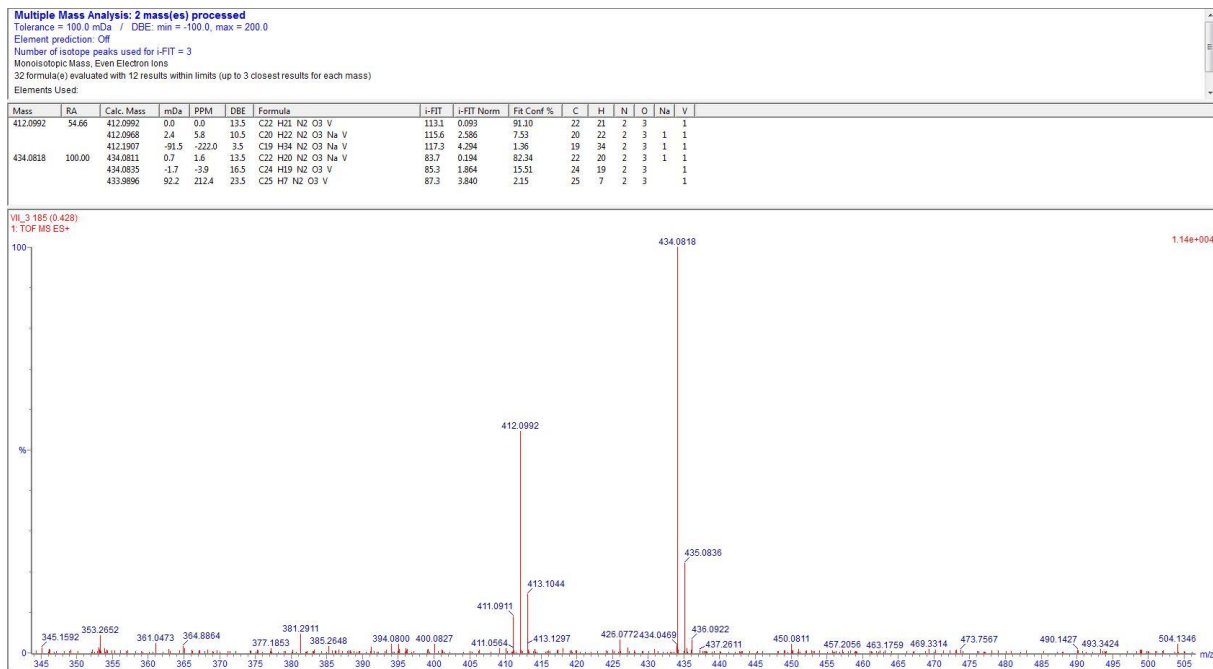


(b)



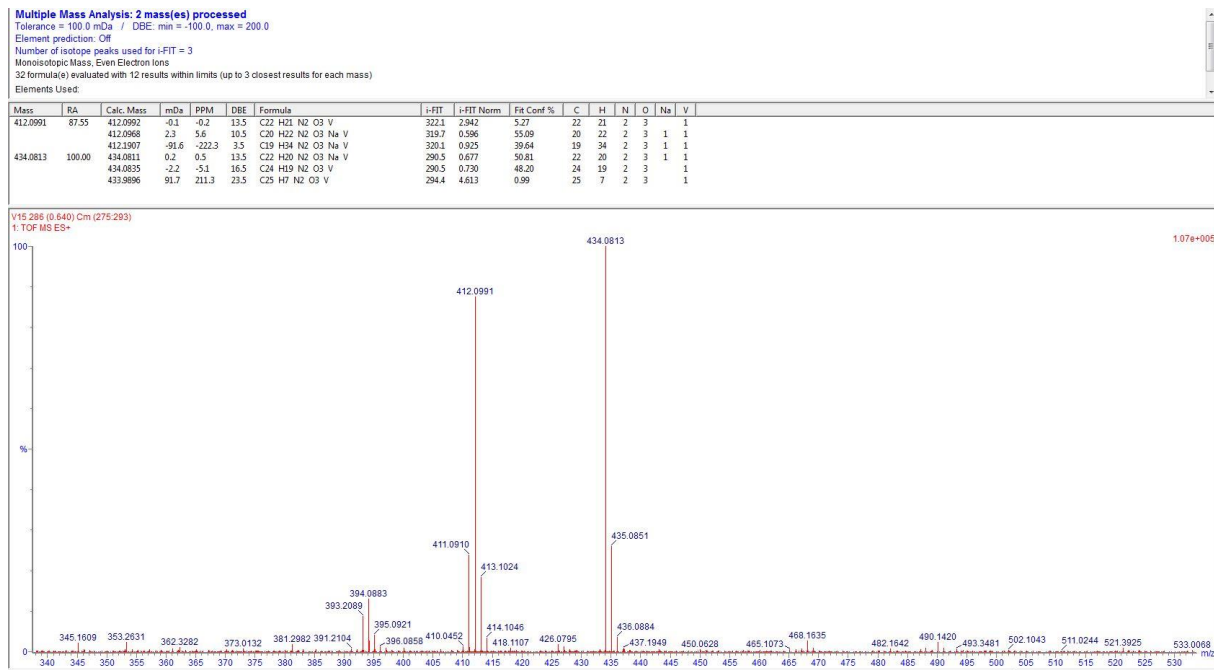
(c)

Figure S1. IR spectra of the complexes **1–3** (blue) and free ligands (red) (a-c).



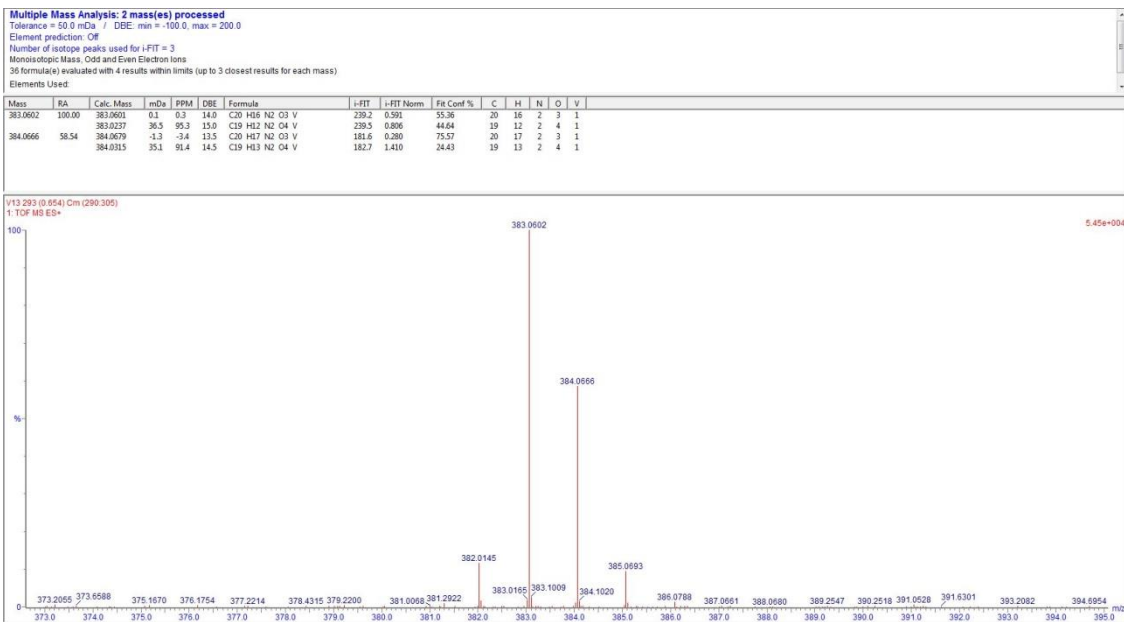
(a)

HRMS (ESI): calcd for C₂₂H₂₀N₂O₃NaV⁺ [M+Na]⁺ 434.0811 found 434.0818.



(b)

HRMS (ESI): calcd for C₂₂H₂₀N₂O₃NaV⁺ [M+Na]⁺ 434.0811 found 434.0813.



(c)

HRMS (ESI): calcd for C₂₀H₁₆N₂O₃V [M]⁺ 383.0601 found 383.0602.

Figure S2. HRMS spectra of the complexes 1–3 (a–c)

X-Ray studies

Table S1. Selected bond lengths (\AA) and angles (deg) for **1**.

Bond lengths		Bond angles	
V(1)–O(1)	1.9210(14)	O(1)a–V(1)–O(1)	125.26(9)
V(1)–O(2)	1.590(2)	O(1)–V(1)–O(2)	117.37(5)
V(1)–N(1)	2.1239(15)	O(1)–V(1)–N(1)	80.51(6)
		O(1)a–V(1)–N(1)	89.93(6)
		O(2)–V(1)–N(1)	100.40(4)
		N(1)–V(1)–N(1)a	159.19(9)

^aSymmetry transformations used to generate equivalent atoms: (a) = $-x, y, 1/2 - z$

Table S2. Selected bond lengths (\AA) and angles (deg) for **2**.

Bond lengths		Bond angles	
V(1)–O(1)	1.924(2)	O(1)–V(1)–O(2)	126.96(11)
V(1)–O(2)	1.917(2)	O(1)–V(1)–O(3)	116.84(11)
V(1)–O(3)	1.595(3)	O(2)–V(1)–O(3)	116.20(12)
V(1)–N(1)	2.122(2)	O(1)–V(1)–N(1)	80.07(9)
V(1)–N(2)	2.125(2)	O(2)–V(1)–N(1)	91.91(9)
		O(3)–V(1)–N(1)	98.56(11)
		O(1)–V(1)–N(2)	90.18(9)
		O(2)–V(1)–N(2)	80.51(10)
		O(3)–V(1)–N(2)	100.85(11)
		N(1)–V(1)–N(2)	160.56(11)

Table S3. Selected bond lengths (\AA) and angles (deg) for **3**.

Bond lengths		Bond angles	
V(1)–O(1)	1.9139(13)	O(1)a–V(1)–O(1)	127.03(9)
V(1)–O(2)	1.588(2)	O(1)–V(1)–O(2)	116.48(5)
V(1)–N(1)	2.1308(16)	O(1)–V(1)–N(1)	80.31(6)
		O(1)a–V(1)–N(1)	91.33(6)
		O(2)–V(1)–N(1)	99.36(4)
		N(1)–V(1)–N(1)a	161.29(9)

Table S4. Short intra- and intermolecular hydrogen bonds.

D–H \cdots A	D–H [\AA]	H \cdots A [\AA]	D–A [\AA]	D–H \cdots A [°]
1				
C(10)–H(10A) \cdots O(1) ^a	0.96	2.56	3.237(3)	128.0
C(2)–H(2) \cdots O(2) ^b	0.93	2.66	3.142(3)	112.9
2				
C(10)–H(10C) \cdots O(2)	0.96	2.50	3.084(4)	119.0
C(21)–H(21C) \cdots O(1)	0.96	2.36	3.185(5)	144.0
C(22)–H(22A) \cdots O(3) ^c	0.96	2.49	3.399(5)	158.0
3				
C(10)–H(10C) \cdots O(1)	0.96	2.33	3.503(15)	145.2

Symmetry codes: (a) = $-x, y, 1/2 - z$; (b) = $-x, 1-y, -z$; (c) = $2-x, 1-y, 2-z$; (d) = $1-x, y, 1/2 - z$

Table S5. Short $\pi \bullet \bullet \bullet \pi$ interactions.

$Cg(I) \bullet \bullet \bullet Cg(J)$	$Cg(I) \cdots Cg(J)$ [Å]	α [°]	β [°]	γ [°]	$Cg(I)$ -Perp [Å]	$Cg(J)$ -Perp [Å]
1						
$Cg(1) \bullet \bullet \bullet Cg(1)^a$	3.5193(12)	0	12.33	12.33	3.4381(8)	3.4381(8)
$Cg(1) \bullet \bullet \bullet Cg(2)^a$	3.9845(13)	0.42(10)	30.38	30.36	3.4382(8)	3.4375(9)
2						
$Cg(1) \bullet \bullet \bullet Cg(2)^b$	3.8928(18)	0.94(15)	29.2	29.1	3.4024(13)	3.3991(13)
$Cg(3) \bullet \bullet \bullet Cg(3)^c$	3.8328(19)	0.00(15)	6.4	6.4	3.8091(13)	3.8090(13)
$Cg(2) \bullet \bullet \bullet Cg(2)^b$	3.7055(19)	0.02(15)	23.9	23.9	3.3885(13)	3.3885(13)
3						
$Cg(4) \bullet \bullet \bullet Cg(4)^b$	3.6285(12)	0	10.77	10.77	3.5645(8)	3.5645(8)

α = dihedral angle between $Cg(I)$ and $Cg(J)$; $Cg(I)$ -Perp = Perpendicular distance of $Cg(I)$ on ring J; $Cg(J)$ -Perp = perpendicular distance of $Cg(J)$ on ring I; β = angle $Cg(I) \rightarrow Cg(J)$ vector and normal to ring I; γ = angle $Cg(I) \rightarrow Cg(J)$ vector and normal to plane J;
 $Cg1$ is the centroid of atoms N(1)/C(1)/C(2)/C(3)/C(4)/C(9); $Cg2$ is the centroid of atoms C(4)/C(5)/C(6)/C(7)/C(8)/C(9); $Cg3$ is the centroid of atoms N(2)/C(12)/C(13)/C(14)/C(15)/C(16); $Cg4$ is the centroid of atoms N(1)/C(1)/C(2)/C(3)/C(4)/C(5);
Symmetry codes: (a) = -x,2-y,-z; (b) = 1-x,1-y,1-z; (c) = 2-x,1-y,2-z

Table S6. X—Y $\bullet \bullet \bullet Cg(J)$ (π -ring) interactions.

$Y-X(I) \bullet \bullet \bullet Cg(J)$	$X(I) \bullet \bullet \bullet Cg(J)$ [Å]	X -Perp [Å]	γ [°]	$Y-X(I) \bullet \bullet \bullet Cg(J)$ [°]
1				
$C(10)-H(10C) \bullet \bullet \bullet Cg(1)^a$	2.91	-2.86	9.70	140.0
2				
$C(10)-H(10B) \bullet \bullet \bullet Cg(3)^b$	2.98	-2.89	14.41	136.0
3				
$C(10)-H(10A) \bullet \bullet \bullet Cg(3)^c$	2.78	-2.73	11.42	165.0

γ = angle $X(I) \rightarrow Cg(J)$ vector and normal to plane J.
 $Cg1$ is the centroid of atoms N(1)/C(1)/C(2)/C(3)/C(4)/C(9); $Cg3$ is the centroid of atoms N(1)/C(1)/C(2)/C(3)/C(4)/C(5);
Symmetry codes: (a) = -x,1-y,-z; (b) = 1-x,1/2+y,3/2-z; (c) = 1-x,-y,1-z;

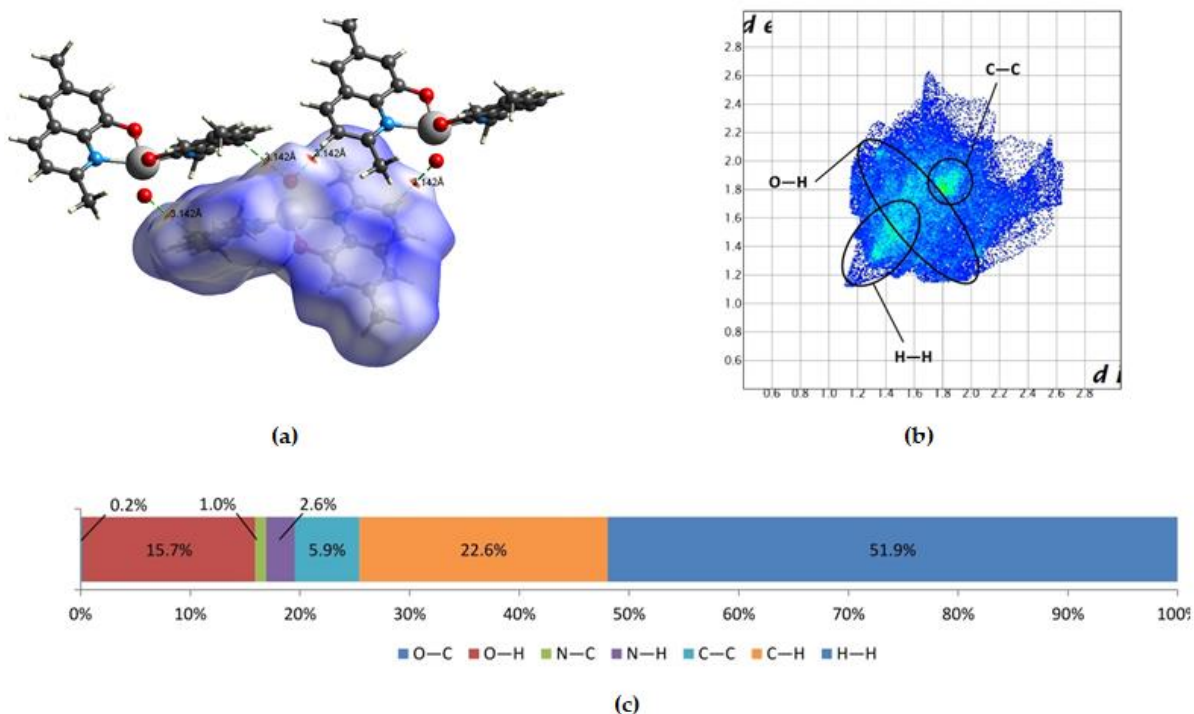


Figure S3. Hirshfeld surface mapped with d_{norm} along with intermolecular hydrogen bonds (a), and 2D fingerprint plot (b) for **1**, together with the relative contributions of various intermolecular interactions to the Hirshfeld surface (c).

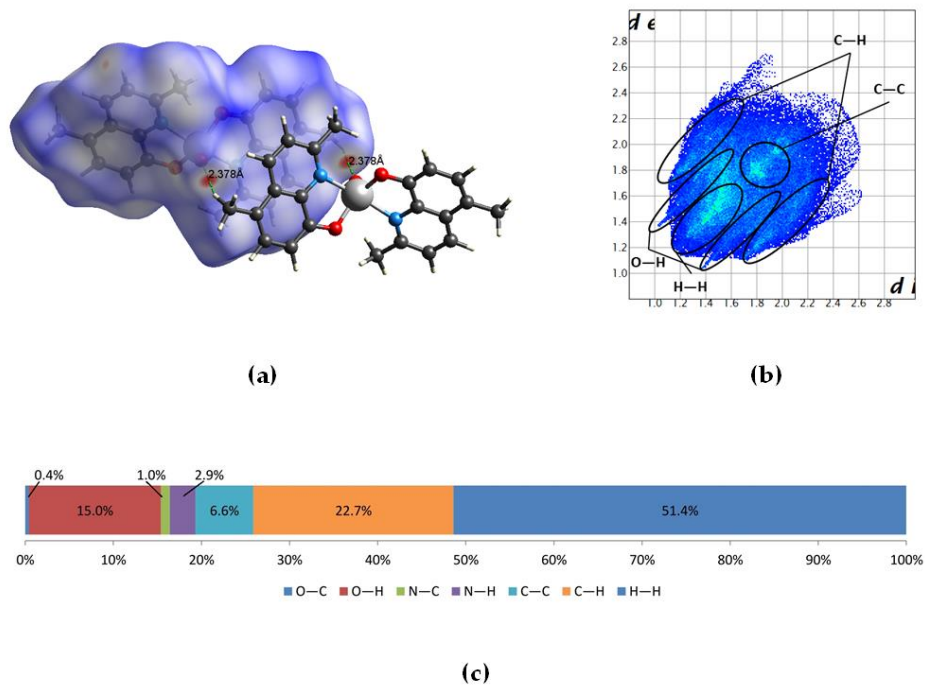


Figure S4. Hirshfeld surface mapped with d_{norm} along with intermolecular hydrogen bonds (a), and 2D fingerprint plot (b) for **2**, together with the relative contributions of various intermolecular interactions to the Hirshfeld surface (c).

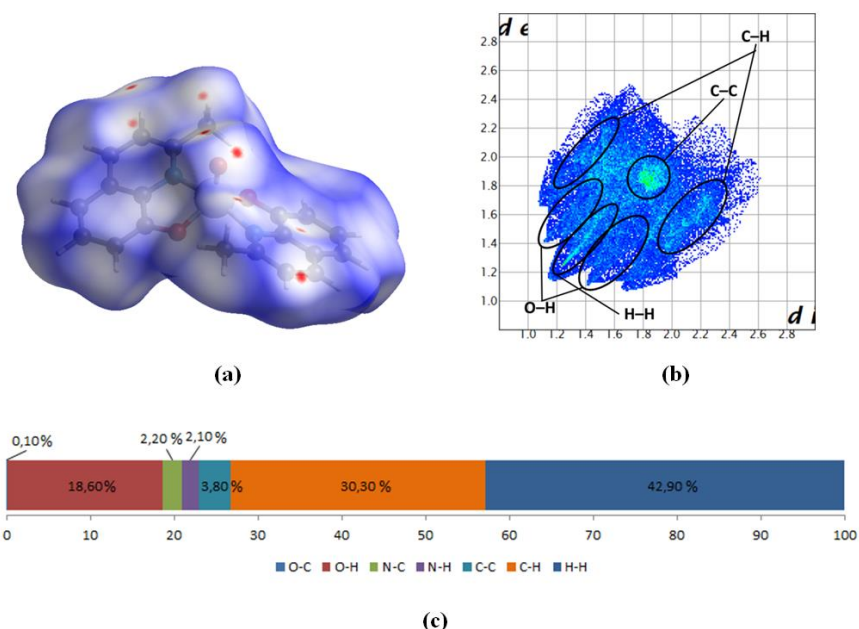
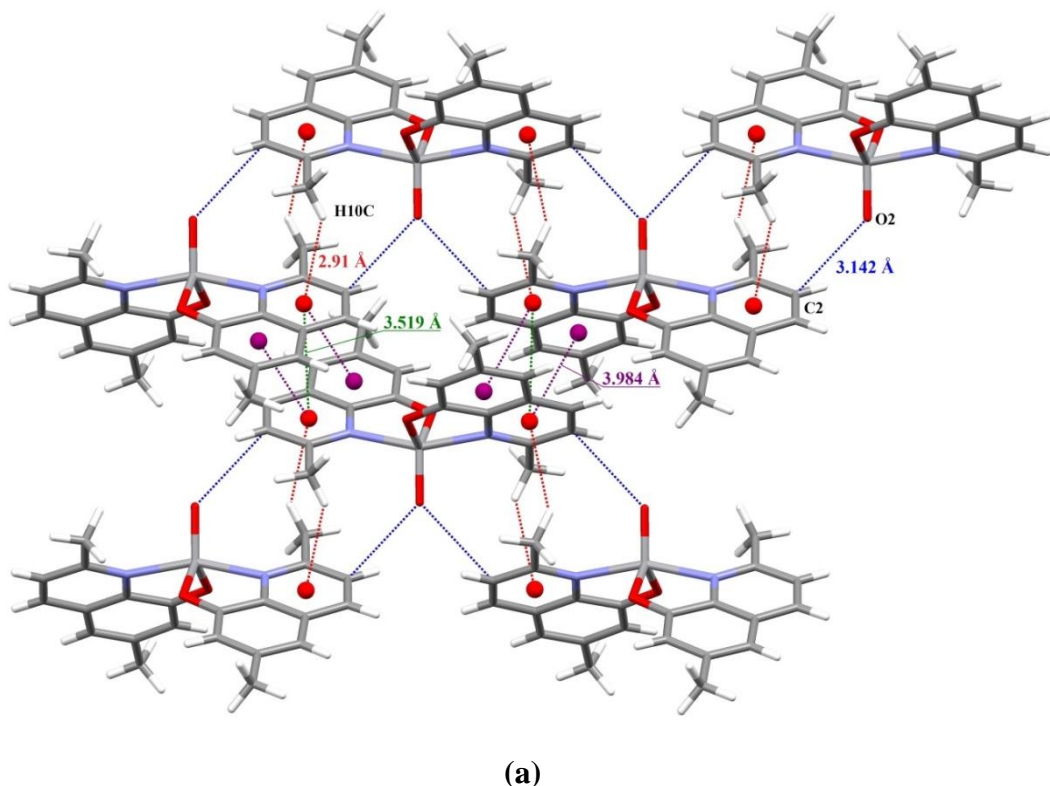
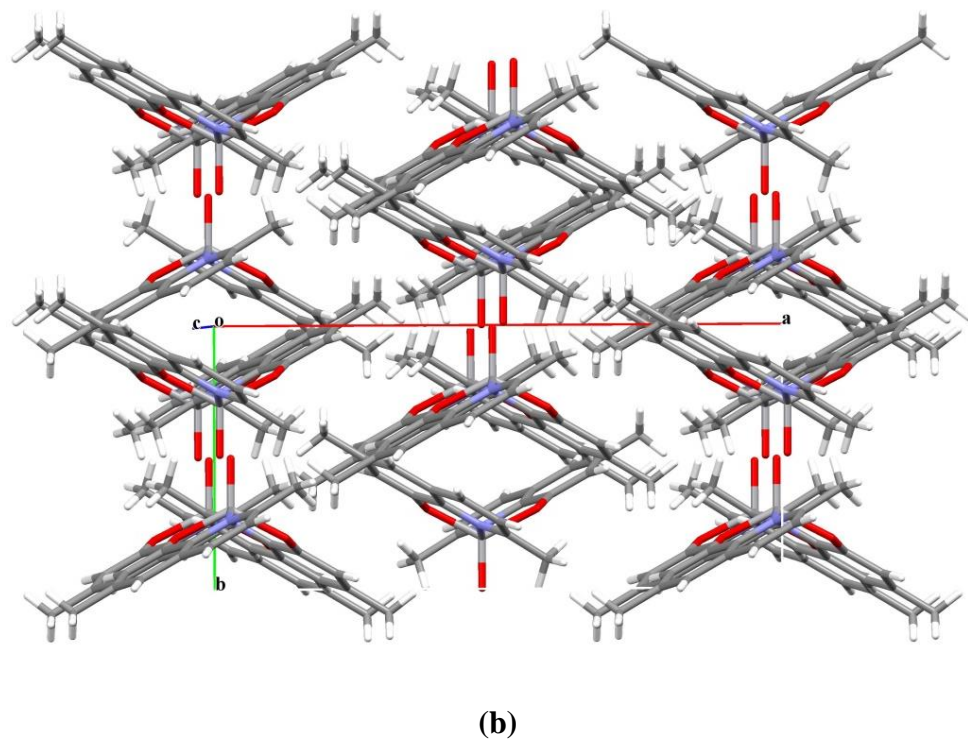


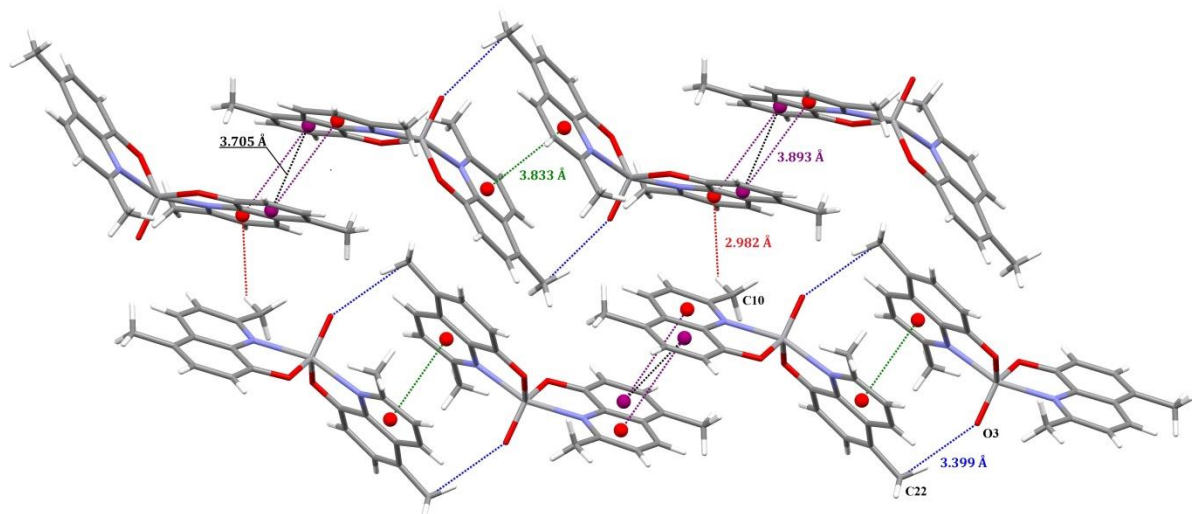
Figure S5. Hirshfeld surface mapped with dnorm along with intermolecular hydrogen bonds (a), and 2D fingerprint plot (b) for 3, together with the relative contributions of various intermolecular interactions to the Hirshfeld surface (c).





(b)

Figure S6. View of the intermolecular interactions ($\pi\bullet\bullet\bullet\pi$, C–H $\bullet\bullet\bullet\pi$ and C–H $\bullet\bullet\bullet$ O) in 1 (a), view of the supramolecular packing of 1 alongside c (b).



(a)

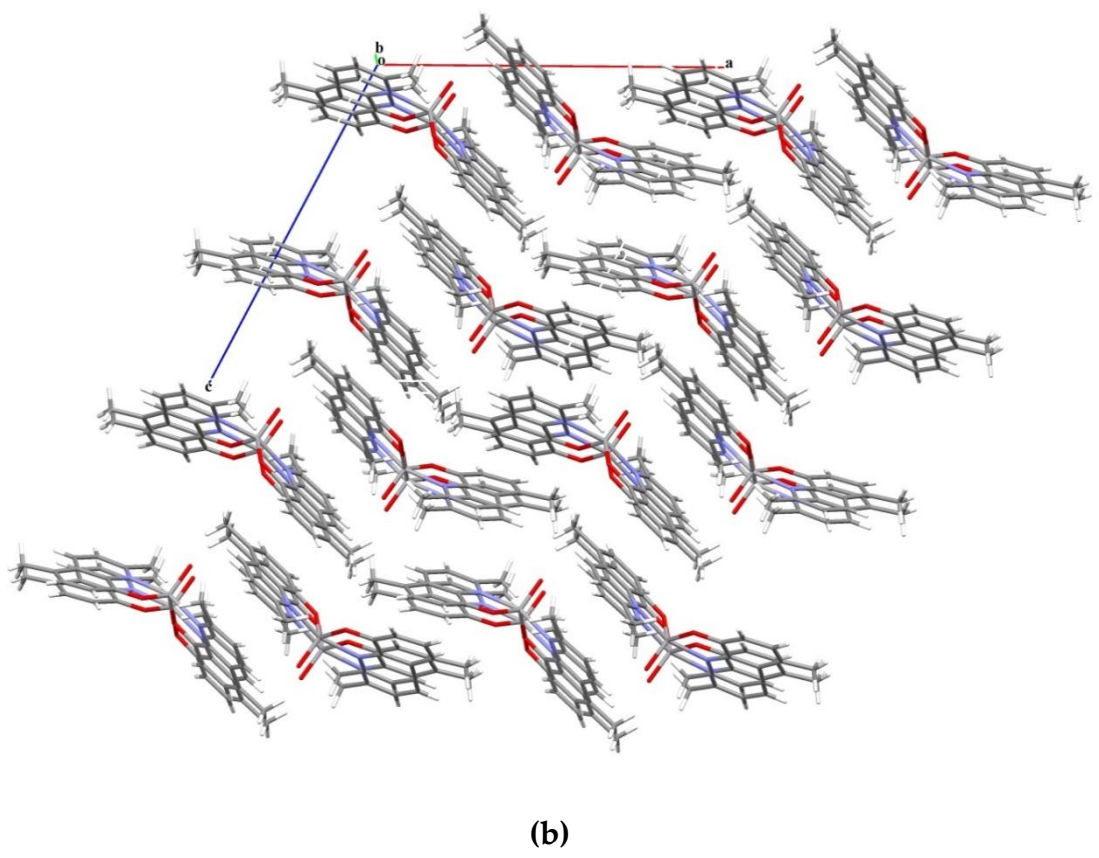
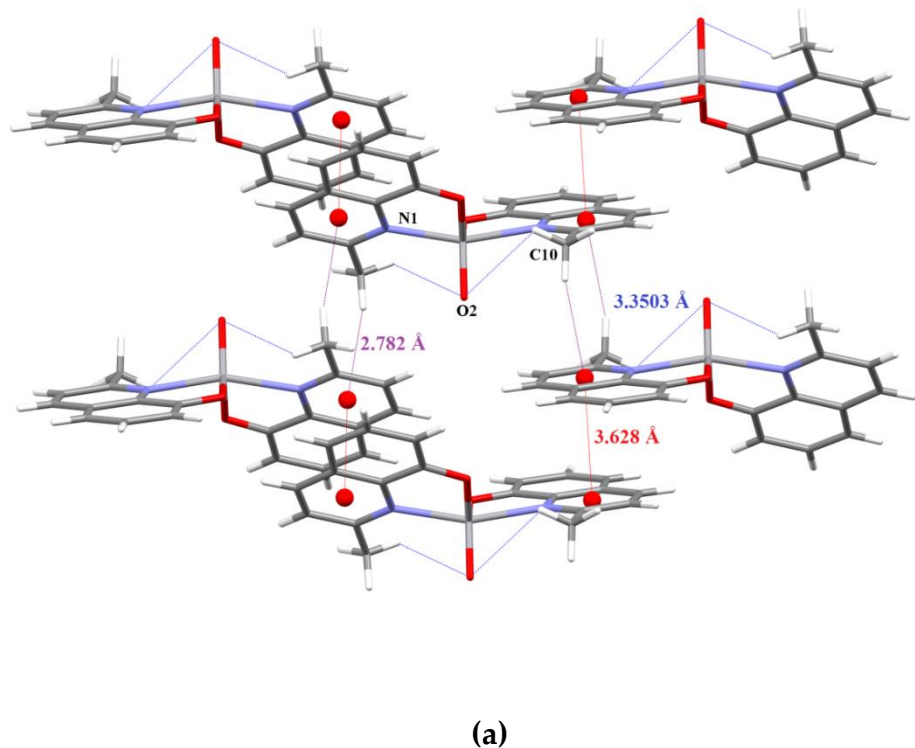


Figure S7. View of the intermolecular interactions ($\pi\bullet\bullet\bullet\pi$, C-H $\bullet\bullet\bullet\pi$ and C-H $\bullet\bullet\bullet$ O) in 2 (a), view of the supramolecular packing of 2 alongside *b* (b).



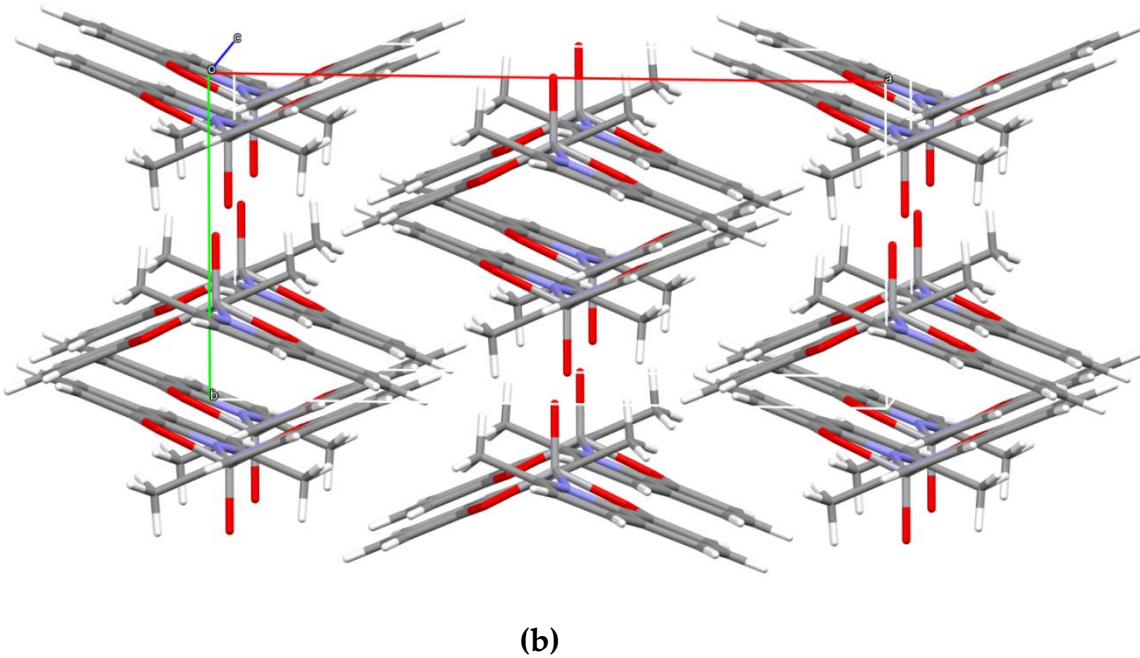
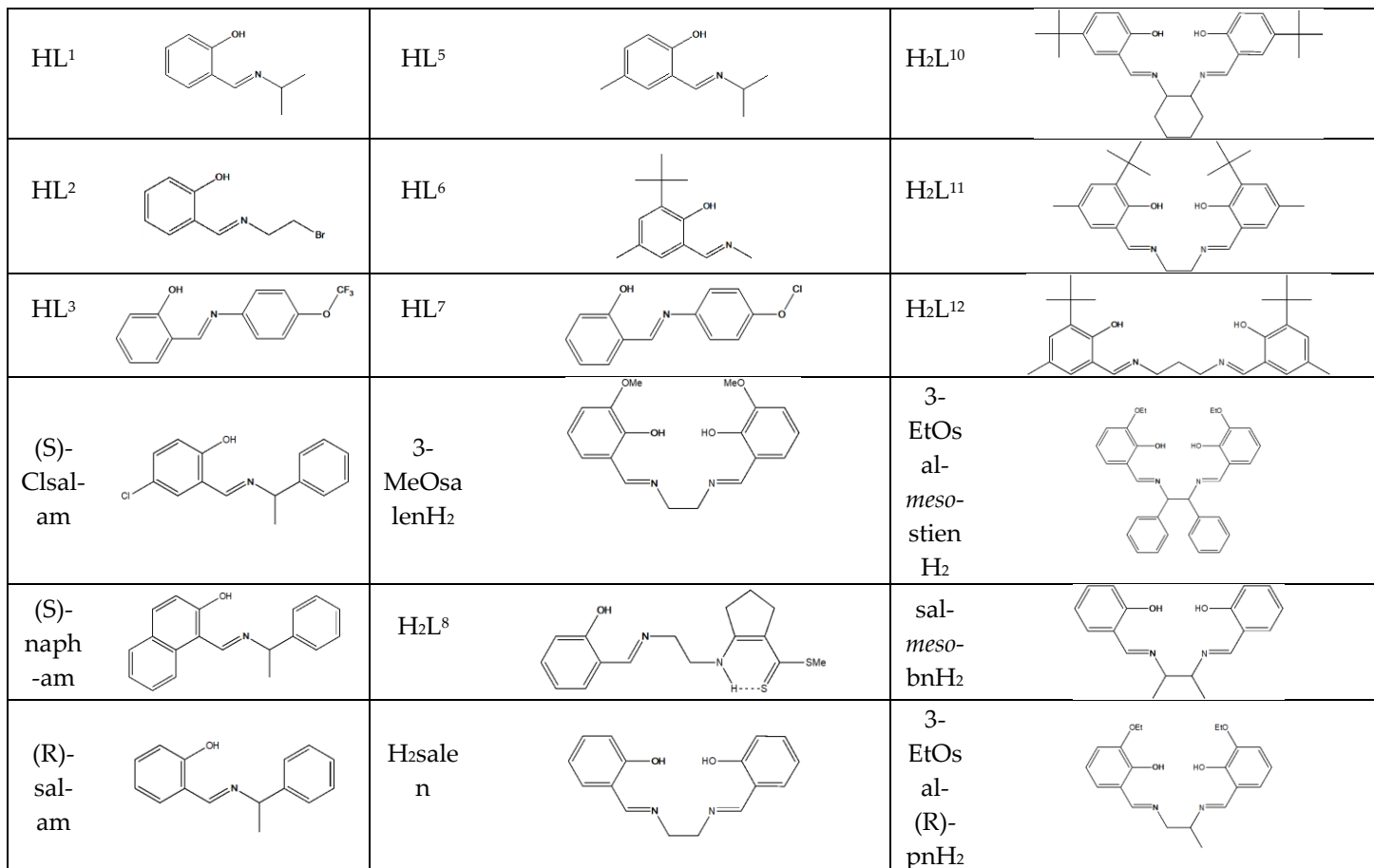


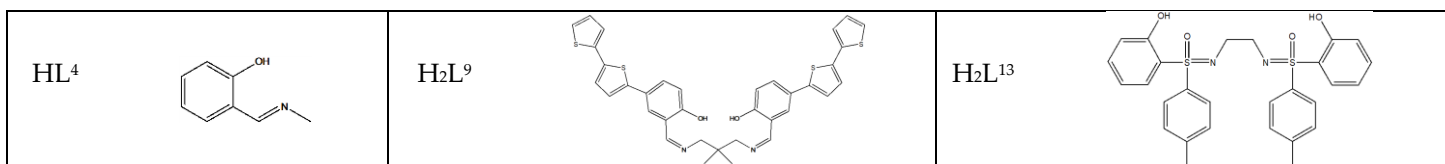
Figure S8. View of the intermolecular interactions ($\pi\bullet\bullet\bullet\pi$, C–H $\bullet\bullet\bullet\pi$ and C–H $\bullet\bullet\bullet$ O) in 3 (a), view of the supramolecular packing of 3 alongside c (b).

Table S7. The selected structural parameters of five-coordinated vanadium(IV) complexes $[\text{VO}(\text{N}^{\wedge}\text{O})_2]$ and $[\text{VO}(\text{O}^{\wedge}\text{N}^{\wedge}\text{N}^{\wedge}\text{O})]$.

Compound	V=O [Å]	V–O [Å]	V–N [Å]	τ	Ref.
$[\text{VO}(\text{N}^{\wedge}\text{O})_2]$					
$[\text{VO}(2,6-(\text{Me})_2\text{-quin})_2]$ (1)	1.590(2)	1.9210(14)	2.1239(15)	0.57	this work
$[\text{VO}(2,5-(\text{Me})_2\text{-quin})_2]$ (2)	1.595(3)	1.924(2); 1.917(2)	2.122(2); 2.125(2)	0.56	this work
$[\text{VO}(2\text{-Me-quin})_2]$	1.600(8)	1.921(5)	2.136(6)	0.56	1
$[\text{VO}(2\text{-Me-5-SMe-quin})_2]$	1.576(6)	1.934(6); 1.923(6)	2.106; 2.122(8)	0.50	2
$[\text{VO}(\text{n-Pr-sal})_2]$	1.5945(18)	1.9042(16); 1.8976(19)	2.126(2); 2.107(2)	0.53	3
$[\text{VO}(\text{L}^1)_2]$	1.587(4)	1.901 (4); 1.914 (3)	2.087 (4); 2.088 (4)	0.58	4
$[\text{VO}(2\text{-OC}_6\text{H}_4\text{CHNH})_2]$	1.589(4)	1.917 (4); 1.919(4)	2.056(6); 2.058(6)	0.22	5
$[\text{VO}(\text{L}^2)_2]$	1.5987(16)	1.9038(16); 1.9194(17)	2.1088(19); 2.1095(18)	0.37	6
$[\text{VO}(\text{L}^3)_2]$	1.589 (2)	1.891(2); 1.904(2)	2.110(2); 2.121(2)	0.42	7
$[\text{VO}\{(\text{S})\text{-Clsal-am}\}_2]\text{C}_7\text{H}_8$	1.592(5)	1.912(4); 1.915(4)	2.076(6); 2.085(6)	0.62	8
$[\text{VO}\{(\text{S})\text{-naph-am}\}_2]$	1.611(2)	1.900(3); 1.904(3)	2.065(3); 2.085(3)	0.75	
$[\text{VO}\{(\text{R})\text{-sal-am}\}_2]\text{C}_7\text{H}_8$	1.592(2)	1.905(2); 1.910(2)	2.112(3); 2.100(3)	0.44	
$[\text{VO}(\text{L}^4)_2]$	1.590(4)	1.893(3)	2.097(3)	0.55	9
$[\text{VO}(\text{L}^5)_2]$	1.5988(18)	1.9117(16); 1.9149(16)	2.096(2); 2.098(2)	0.58	
$[\text{VO}(\text{L}^6)_2]$	1.601(2)	1.9005(17);	2.076(2); 2.089(2)	0.70	

		1.9027(16)			
[VO(L ⁷) ₂]	1.615(8)	1.902(7); 1.900(8)	2.153(9); 2.145(9)	0.43	10
[VO(O ⁷ N ⁷ N ⁷ O)]					
[VO(3-MeOsalen)] ·H ₃ N(CH ₂) ₂ NH ₂ Cl	1.5938(18)	1.9228(16); 1.9287(17)	2.047(2); 2.051(2)	0.13	11
<i>syn</i> -[VO(HL ⁸) ₂]	1.596(6)	1.914(4)	2.100(4)	0.55	12
<i>anti</i> -[VO(HL ⁸) ₂]	1.577(4)	1.763(3); 1.896(3)	2.064(3); 2.189(3)	0.06	
[VO(salen)]·MeOH	1.6070 (17)	1.9155 (17); 1.9429 (16)	2.051 (2); 2.0597 (19)	0.20	13
[VOL ⁹]·MeCN	1.610(5)	1.961(5); 1.972(5)	2.091(6); 2.093(6)	0.03	14
[VOL ¹⁰]·CHCl ₃	1.606(2)	1.921(2); 1.922(2)	2.060(3); 2.072(3)	0.29	15
[VOL ¹¹]·CHCl ₃	1.5913(13)	1.9226(12); 1.9351(12)	2.0589(15); 2.0710(15)	0.26	9
[VOL ¹²]	1.581(3)	1.937(3); 1.954(3)	2.095(3); 2.100(3)	0.30	
[VO(3-EtOsal- <i>meso</i> -stien)]·H ₂ O	1.597(3)	1.925(3); 1.934(2)	2.065(3); 2.072(3)	0.05	16
[VO(sal- <i>meso</i> -bn)]	1.595(2)	1.937(2); 1.948(2)	2.061(2); 2.068(2)	0.04	17
[VO(salen)]ClO ₄	1.576(3)	1.795(3); 1.813(3)	2.074(3), 2.083(3)	0.01	18
[VO{3-EtOsal-(R)-pn}]	1.598(3)	1.918(3); 1.938(3)	2.066(4); 2.053(4)	0.11	19
[VOL ¹³]	1.585(3)	1.924(3); 1.938(3)	2.050(3); 2.055(3)	0.12	20
[VO(salen)BF ₄]	1.577(2)	1.794(2); 1.814(2)	2.067(2); 2.085(2)	0.01	21





References to table:

- Shiro M.; Fernando, Q. Structures of two five-coordinated metal chelates of 2-methyl-8-quinolinol. *Anal. Chem.* **1971**, *43*, 1222–1230.
- Groom, C. R.; Bruno, I. J.; Lightfoot M. P.; Ward, S. C. The Cambridge structural database. *Acta Cryst.* **2016**, *B72*, 171–179
- Elias, H.; Schwartz-Eidam, S.; Wannowius, K. J. Kinetics and mechanism of ligand substitution in bis(*N*-alkylsalicylaldiminato)oxovanadium(IV) complexes. *Inorg. Chem.* **2003**, *42*, 2878–2885.
- Menati, S.; Rudbari, H. A.; Khorshidifar M.; Jalilian, F. A new oxovanadium(IV) complex containing an O,N-bidentate Schiff base ligand: Synthesis at ambient temperature, characterization, crystal structure and catalytic performance in selective oxidation of sulfides to sulfones using H_2O_2 under solvent-free conditions. *J. Mol. Struct.*, **2016**, *1103*, 94–102.
- Choudhary, N.; Hughes, D. L.; Kleinkes, U.; Larkworthy, L. F.; Leigh, G. J.; Maiwald, M.; Marmion, C. J.; Roger Sanders, J.; Smith G. W.; Sudbrake, C. New tetradeятate Schiff bases, their oxovanadium (IV) complexes, and some complexes of bidentate Schiff bases with vanadium (III). *Polyhedron* **1997**, *16*, 1517–1528
- Grivani, G.; Khalaji, A. D.; Tahmasebi, V.; Gotoh K.; Ishida, H. Synthesis, characterization and crystal structures of new bidentate Schiff base ligand and its vanadium(IV) complex: The catalytic activity of vanadyl complex in epoxidation of alkenes. *Polyhedron* **2012**, *31*, 265–271.
- Burgess, J.; Fawcett, J.; Palma V.; Gilani, S. R. Fluoro derivatives of bis(salicylideneaminato-N, O) copper (II) and-oxovanadium (IV). *Acta Cryst.* **2001**, *C57*, 277–280.
- Santoni G.; Rehder, D. Structural models for the reduced form of vanadate-dependent peroxidases: vanadyl complexes with bidentate chiral Schiff base ligands. *J. Inorg. Biochem.* **2004**, *98*, 758–764.
- Cornman, C. R.; Geiser-Bush, K. M.; Rowley, S. P.; Boyle, P. D. Structural and Electron Paramagnetic Resonance Studies of the Square Pyramidal to Trigonal Bipyramidal Distortion of Vanadyl Complexes Containing Sterically Crowded Schiff Base Ligands. *Inorg. Chem.* **1997**, *36*, 6401–6408.
- Pasquali, M.; Marchetti, F.; Floriani C.; Merlini, S. Oxovanadium(IV) complexes containing bidentate Schiff-base ligands: synthesis and structural and spectroscopic data. *J. Chem. Soc., Dalton Trans.* **1977**, 139–144.
- Cashin, B.; Cunningham, D.; Daly, P.; McArdle, P.; Munroe M.; Chonchubhair, N. N. Donor properties of the vanadyl ion: Reactions of vanadyl salicylaldimine β -ketimine and acetylacetone complexes with groups 14 and 15 Lewis acids. *Inorg. Chem.* **2002**, *41*, 773–782.
- Bhattacharyya, S.; Mukhopadhyay, S.; Samanta, S.; Weakley, T. J. R.; Chaudhury, M.; Synthesis, characterization, and reactivity of mononuclear O,N-chelated vanadium(IV) and -(III) complexes of methyl 2-aminocyclopent-1-ene-1-dithiocarboxylate based ligand: Reporting an example of conformational isomerism in the solid state. *Inorg. Chem.* **2002**, *41*, 2433–2440
- Hsuan, R. E.; Hughes, J. E.; Miller, T. H.; Shaikh, N.; Cunningham, P. H. M.; O'Connor, A. E.; Tidey J. P.; Blake, A. J. Crystal structure of $\{\text{2,2}'\text{-[ethylenebis(nitrilomethanylidene)]diphenolato-}\text{^{4+},N,N',O'}\}\text{oxidovanadium(IV)}$ methanol monosolvate. *Acta Cryst.* **2014**, *E70*, m380–m381.
- Nguyen, M. T.; Jones R. A.; Holliday, B. J. Effect of conjugation length and metal-backbone interactions on charge transport properties of conducting metallocopolymers. *Polym. Chem.* **2017**, *8*, 4359–4367.
- Carter, E.; Fallis, I. A.; Kariuki, B. M.; Morgan, I. R.; Murphy D. M.; Tatchell, T.; Van Doorslaer S.; Vinck, E. Structure and pulsed EPR characterization of *N,N'*-bis(5-*tert*-butylsalicylidene)-1,2-cyclohexanediamino-vanadium(IV) oxide and its adducts with propylene oxide. *Dalton Trans.*, **2011**, *40*, 7454–7462.

16. Hoshina, G.; Tsuchimoto, M.; Ohba, S.; Nakajima, K.; Uekusa, H.; Ohashi, Y.; Ishida H.; Kojima, M. Thermal dehydrogenation of oxovanadium(IV) complexes with schiff base ligands derived from *meso*-1,2-diphenyl-1,2-ethanediamine in the solid state. *Inorg. Chem.* **1998**, *37*, 142–145.
17. Hoshina, G.; Tsuchimoto M.; Ohba, S. *exo*-[(*RS,SR*)-*N,N'*-Bis(salicylidene)-2,3-butanediaminato]oxovanadium(IV) *Acta Cryst.* **1999**, C55, 1082–1084.
18. Bonadies, J. A.; Butler, W. M.; Pecoraro V. L.; Carrano, C. J. Novel reactivity patterns of (*N,N'*-ethylenebis (salicylideneaminato)) oxovanadium (IV) in strongly acidic media. *Inorg. Chem.* **1987**, *26*, 1218–1222.
19. Hoshina, G.; Tsuchimoto M.; Ohba, S. *endo*-{6,6'-Diethoxy-2,2'-[(*R*)-propane-1,2-diylbis(nitrilomethylidene)]diphenolato-*O,N,N',O'*}oxovanadium(IV), *Acta Cryst.* **1999**, C55, 1812–1813.
20. Bolm, C.; Bienewald F.; Harms, K. Syntheses and vanadium complex of salen-like bisulfroximines, *Synlett*, **1996**, *8*, 775–776.
21. Oyaizu, K.; Dewi, E. L.; Tsuchida, E. Coordination of BF_4^- to Oxovanadium(V) Complexes, Evidenced by the Redox Potential of Oxovanadium(IV/V) Couples in CH_2Cl_2 . *Inorg. Chem.* **2003**, *42*, 1070–1075.

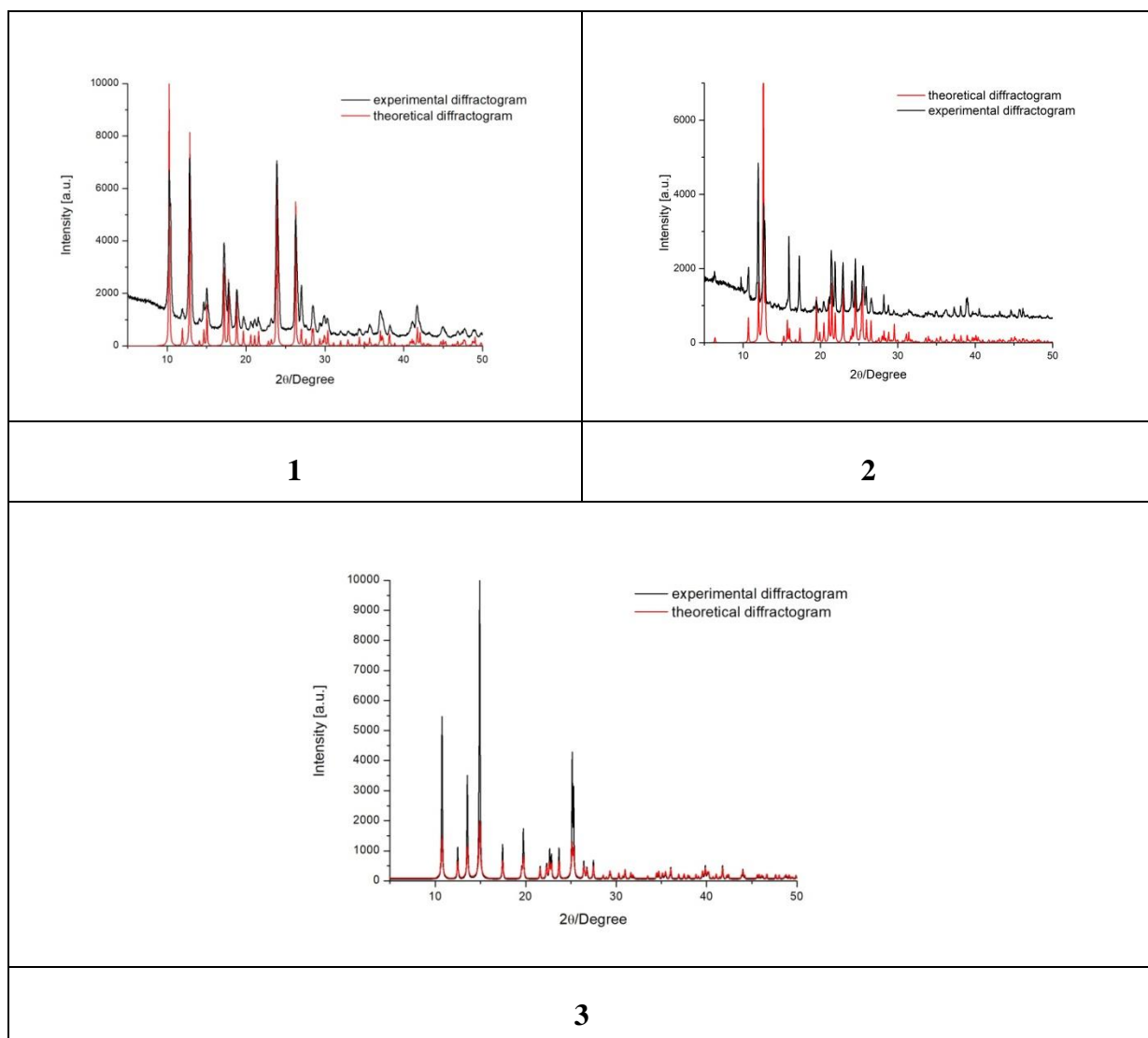


Figure S9. X-ray powder diffraction pattern of **1–3** together with the calculated pattern from the single crystal data.

EPR spectra

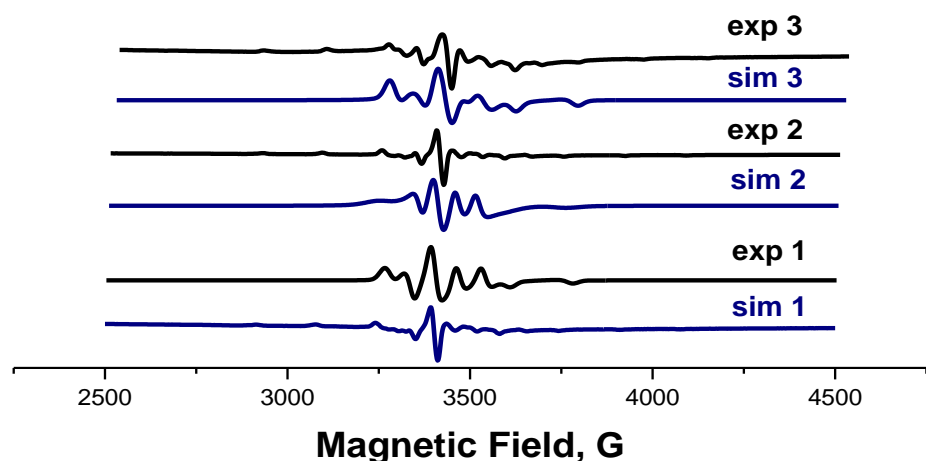
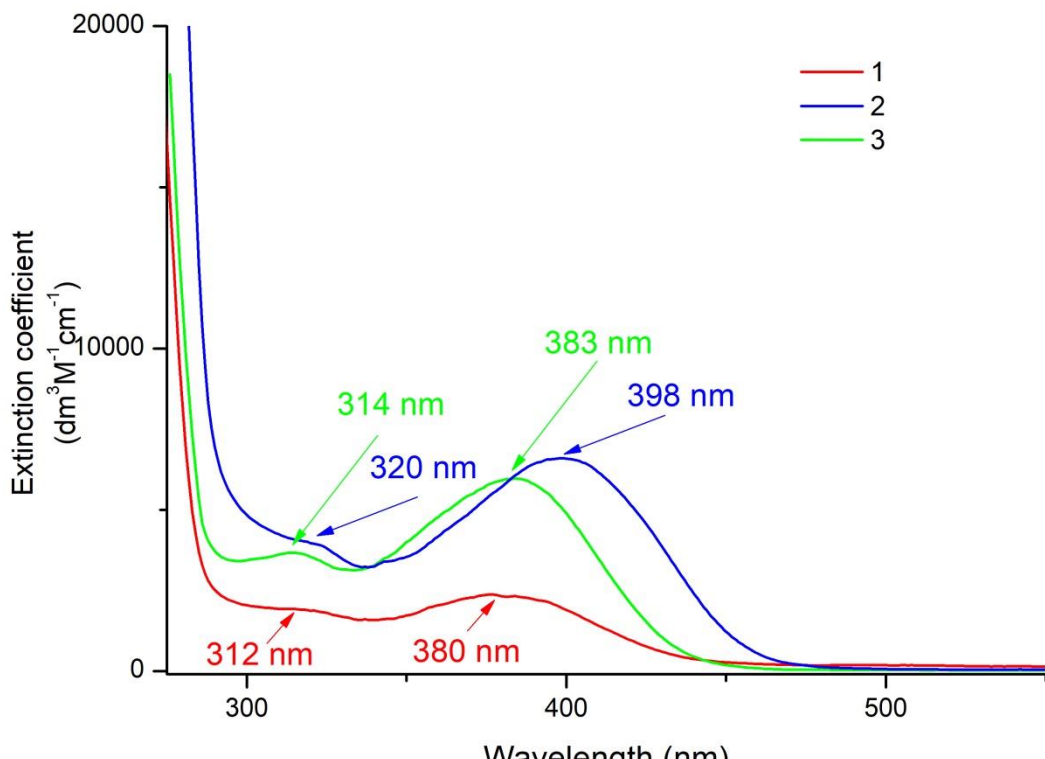
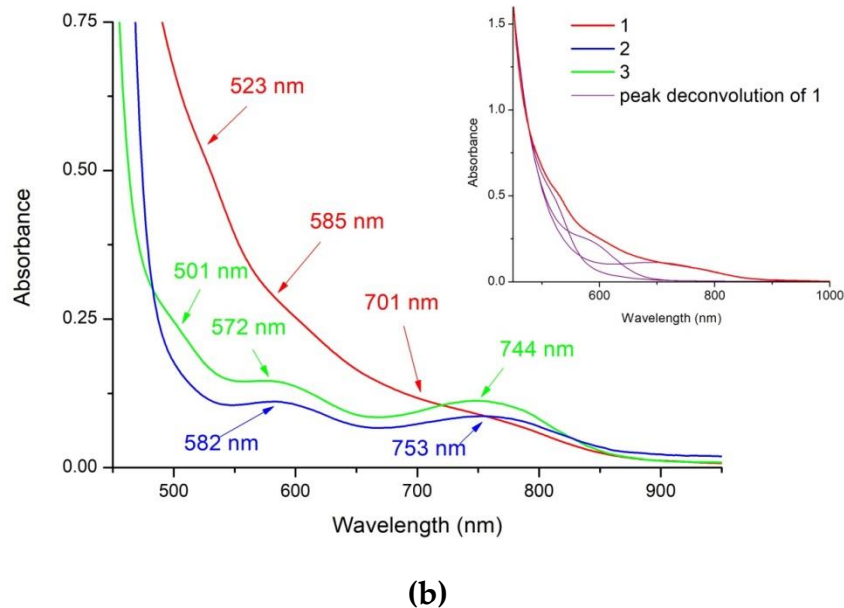


Figure S10. EPR frozen solution spectra (at 77 K) of compounds **1–3**; in acetonitrile solvent together with the theoretical spectrum calculated using the parameters: $g_x = g_y = 1.980$, $g_z = 1.942$, $A_x = A_y = 65$ G, $A_z = 181$ G for **1** and $g_x = g_y = 1.979$, $g_z = 1.957$, $A_x = A_y = 53$ G, $A_z = 169$ G for **2**; $g_x = g_y = 1.978$, $g_z = 1.959$, $A_x = A_y = 55$ G, $A_z = 168$ G for **3**

Absorption spectroscopy



(a)



(b)

Figure S11. UV-Vis spectra of **1–3** in DMSO full scale ($5\cdot10^{-5}$ M) (a), close-up of the 500–900 nm region (concentrated solutions in DMSO) (b), insert: peak deconvolution of **1** calculated using deconvolution formula implemented in the OriginPro 9.1 software

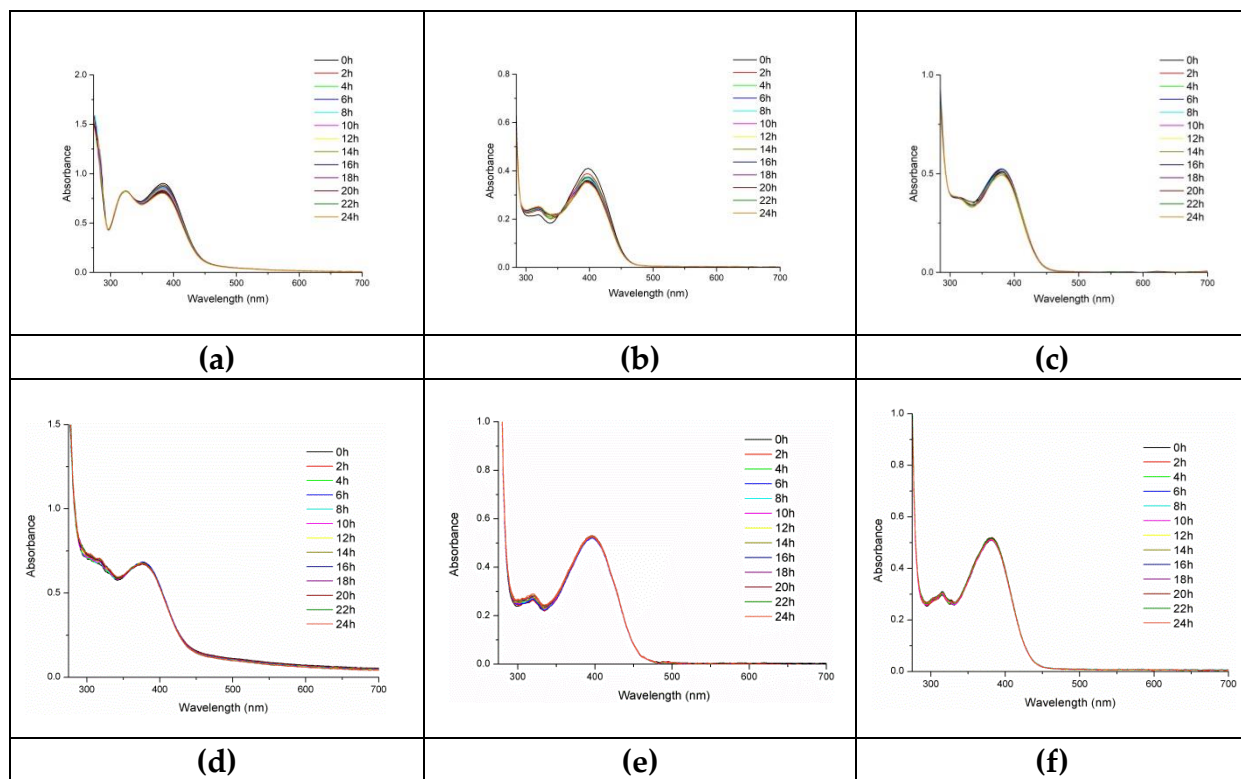


Figure S12. UV-Vis stability spectra for compounds **1–3** in DMSO (10^{-4} M) (a-c) and CH₃CN (d-f). Spectra were recorded every 2 hours for 24h.

Catalytic data

Table S8. Comparative parameters for the oxidation of cyclohexane catalyzed by complexes 1-3 and other vanadium complexes previously published

Catalytic system	Conditions	Vanadium oxidation state	Total yield of oxygenates (%)	Total TON	Ref.
[n-Bu4N][VO ₃]/pca/H ₂ O ₂ /CH ₃ CN	40 °C, 4 h	V	30	700	1
[n-Bu4N][VO ₂ (pca) ₂]/H ₂ O ₂ /CH ₃ CN	40 °C, 24 h	V	4.6	215	2
[n-Bu4N][VO ₂ (pca) ₂]/pca/H ₂ O ₂ /CH ₃ CN	40 °C, 24 h	V	20	900	
[VO(OCH ₃)(ma)2] Hma – 3-hydroxy-2-methyl-4-pyrone	40°C, 14 h	V	27	2600	3
[VO(tea)] tea – triethanolamine	40 °C, 24 h	V	10	900	4
[VO(OCH ₃)(5-Cl-quin) ₂ · 1/2CHCl ₃]/pca/H ₂ O ₂ /CH ₃ CN 5-Cl-quin – 5-chloro-8-hydroxyquinoline	40°C, 6 h	V	39	360	5
[{VO(Oet)(EtOH)} ₂ L]/pca/H ₂ O ₂ /CH ₃ CN H ₄ L – bis(2-hydroxybenzylidene)terephthalohydrazide	50 °C, 24 h	V	30	700	6
[{VO(Oet)(EtOH)} ₂ L]/pca/H ₂ O ₂ /CH ₃ CN H ₄ L – bis(2-hydroxybenzylidene)oxalohydrazonic acid	50 °C, 4 h	V	28.7	2640	7
[VO ₂ (pca)(hmpa)]/pca/H ₂ O ₂ /CH ₃ CN hmpa – hexamethylphosphoramide	40 °C, 24 h	V	29.8	1370	8
[VO ₂ (pycaH)(hmpa)]/pca/H ₂ O ₂ /CH ₃ CN hmpa – hexamethylphosphoramide pycaH ₂ – pyridine-2,5-dicarboxylic acid	40 °C, 24 h	V	24.8	1140	
[{VO ₂ }(μ ⁴ -L){Na ₂ (μ-H ₂ O) ₂ (H ₂ O) ₂ }] _n /pca/H ₂ O ₂ /CH ₃ CN H ₄ L – bis(salicylaldehyde)-oxaloyldihydrazone	50 °C, 5 h	V	4.8	4400	9
[{V(μ-O) ₂ }(μ ⁴ -L){K ₂ (μ-H ₂ O) ₂ (H ₂ O) ₂ }] _n /pca/H ₂ O ₂ /CH ₃ CN H ₄ L – bis(salicylaldehyde)-oxaloyldihydrazone	50 °C, 5 h	V	5.7	5220	
[{V(μ-O)(μ ³ -O)} ₂ (μ ⁵ -L){Cs ₂ (μ-H ₂ O) ₂ (H ₂ O) ₂ }] _n /pca/H ₂ O ₂ /CH ₃ CN H ₄ L – bis(salicylaldehyde)-oxaloyldihydrazone	50 °C, 5 h	V	6.2	5700	
V ₃ O ₉ (Oet)(ashz) ₂ (μ-Oet) ₂ /pca/H ₂ O ₂ /CH ₃ CN H ₃ ashz – N-acetyl salicylyhydrazide	50 °C, 5 h	mixed IV/V	18.2	8370	10
[(VO) ₄ (hptb) ₂ (H ₂ O) ₂ (μ-O)][ClO ₄]/pca/H ₂ O ₂ /CH ₃ CN hptbH – N,N,N',N'-tetrakis(2-benzimidazolylmethyl)-2-hydroxo-1,3-diaminopropane	40 °C, 24 h	IV	12.4	570	8
[VOCl ₂ (tmtacn)]/pca/H ₂ O ₂ /CH ₃ CN tmtacn – 1,4,7-trimethyl-1,4,7-triaza cyclononane	40 °C, 24 h	IV	6.3	290	
[V(cat) ₃]/pca/H ₂ O ₂ /CH ₃ CN catH ₂ – pyro-cathecol	40 °C, 24 h	IV	21.3	980	
[VOCl ₂ (dpp-bian)]/pca/H ₂ O ₂ / CH ₃ CN dpp-bian – bis(N-(2,6-diisopropylphenyl)-imino)acenaphthene	50 °C, 5 h	IV	21.5	990	11
VO(acac) ₂ /H ₂ O ₂ / CH ₃ CN	40°C, 5 h	IV	1.2	23	12,13
1/pca/ H ₂ O ₂ /CH ₃ CN	50 °C, 3 h	IV	30	565	this work
2/pca/ H ₂ O ₂ /CH ₃ CN	50 °C, 2 h	IV	43	870	
3/pca/ H ₂ O ₂ /CH ₃ CN	50 °C, 1.5 h	IV	48	954	

References to table:

1. Shul'pin, G. B.; Attanasio, D.; Suber, L. Efficient H₂O₂ oxidation of alkanes and arenes to alkyl peroxides and phenols catalyzed by the system vanadate–pyrazine-2-carboxylic acid. *J. Catal.* **1993**, *142*, 147–152.
2. Süss-Fink, G.; Stanislas, S.; Shul'pin, G. B.; Nizova, G. V.; Stoeckli-Evans, H.; Neels, A.; Bobillier, C.; Claude, S.; Oxidative functionalisation of alkanes: synthesis, molecular structure and catalytic implications of anionic vanadium(V) oxo and peroxy complexes containing bidentate N,O ligands. *J. Chem. Soc., Dalton Trans.* **1999**, 3169–3175.
3. Shul'pin, G. B.; Mishra, G. S.; Shul'pina, L. S.; Strelkova, T. V.; Pombeiro, A. J. L. Oxidation of hydrocarbons with hydrogen peroxide catalyzed by maltolato vanadium complexes covalently bonded to silica gel. *Catal. Commun.* **2007**, *8*, 1516–1520.
4. Kirillova, V.; Kuznetsov, M. L.; Romakh, V. B.; Shul'pina, L. S.; Fraústo da Silva, J. J. R.; Pombeiro, A. J. L.; Shul'pin, G. B. Mechanism of oxidations with H₂O₂ catalyzed by vanadate anion or oxovanadium(V) triethanolamine (vanadatrane) in combination with pyrazine-2-carboxylic acid (PCA): Kinetic and DFT studies. *J. Catal.* **2009**, *267*, 140–157.
5. Sutradhar, M.; Shvydkiy, N. V.; da Silva, M. F. C. G.; Kirillova, M. V.; Kozlov, Y. N.; Pombeiro, A. J. L.; Shul'pin, G. B. New binuclear oxovanadium(V) complex as a catalyst in combination with pyrazinecarboxylic acid (PCA) for efficient alkane oxygenation by H₂O₂. *Dalton Trans.*, **2013**, *42*, 11791–11803.
6. Sutradhar, M.; Shvydkiy, N. V.; Guedes da Silva, C. F. M.; Kirillova, M. V.; Kozlov, Y. N.; Pombeiro, A. J. L.; Shul'pin, G. B. A new binuclear oxovanadium(v) complex as a catalyst in combination with pyrazinecarboxylic acid (PCA) for efficient alkane oxygenation by H₂O₂. *Dalton Trans.*, **2013**, *42*, 11791–11803.
7. Gupta, S.; Kirillova, M. V.; Guedes da Silva, M. F.; Pombeiro, A. J. L., Highly efficient divanadium(V) pre-catalyst for mild oxidation of liquid and gaseous alkanes. *Appl. Catal. A-Gen.*, **2013**, *460*-461, 82–89.
8. Süss-Fink, G.; Gonzalez Cuervo, L.; Therrien, B.; Stoeckli-Evans, H.; Shul'pin, G. B. Mono and oligonuclear vanadium complexes as catalysts for alkane oxidation: synthesis, molecular structure, and catalytic potential. *Inorg. Chim. Acta*, **2004**, *357*, 475–484.
9. Gupta, S.; Kirillova, M. V.; Guedes da Silva, M. F. C.; Pombeiro, A. J. L.; Kirillov, A. M. Alkali metal directed of heterometallic V^v/M (M = Na, K, Cs) coordination polymers: structures, topological analysis, and oxidation catalytic properties. *Inorg. Chem.* **2013**, *52*, *15*, 8601–8611.
10. Sutradhar, M.; Kirillova, M. V.; Guedes da Silva, M. F. C.; Martins, L. M. D. R. S; Pombeiro, A. J. L. A hexanuclear mixed-valence oxovanadium(IV,V) complex as a highly efficient alkane oxidation catalyst. *Inorg. Chem.* **2012**, *51*, 11229–11231.
11. Fomenko, I. S.; Gushchin, A. L.; Shul'pina, L. S.; Ikonnikov, N. S.; Abramov, P. A.; Romashev, N. F.; Poryvaev, A. S.; Sheveleva, A. M.; Bogomyakov, A. S.; Shmelev, N. Y.; Fedin, M. V.; Shul'pin, G. B.; Sokolov, M. N. New oxidovanadium(iv) complex with a BIAN ligand: synthesis, structure, redox properties and catalytic activity. *New J. Chem.*, **2018**, *42*, 16200–16210.
12. Pokutsa, A.; Bloniarz, P.; Fliunt, O.; Kubaj, Y.; Zaborovskyi, A.; Pacześniak, T. Sustainable oxidation of cyclohexane catalyzed by a VO(acac)₂-oxalic acid tandem: the electrochemical motive of the process efficiency. *RSC Adv.* **2020**, *10*, 10959–10971.
13. Pokutsa, A.; Kubaj, Y.; Zaborovskyi, A.; Sobkowiak, A., Muzart, J. Oxalic acid-improved mild cyclohexane oxidation catalyzed by VO(acac)₂: non-radical versus radical mechanism. *Reac. Kinet. Mech. Cat.* **2017**, *122*, 757–774.

Biological results

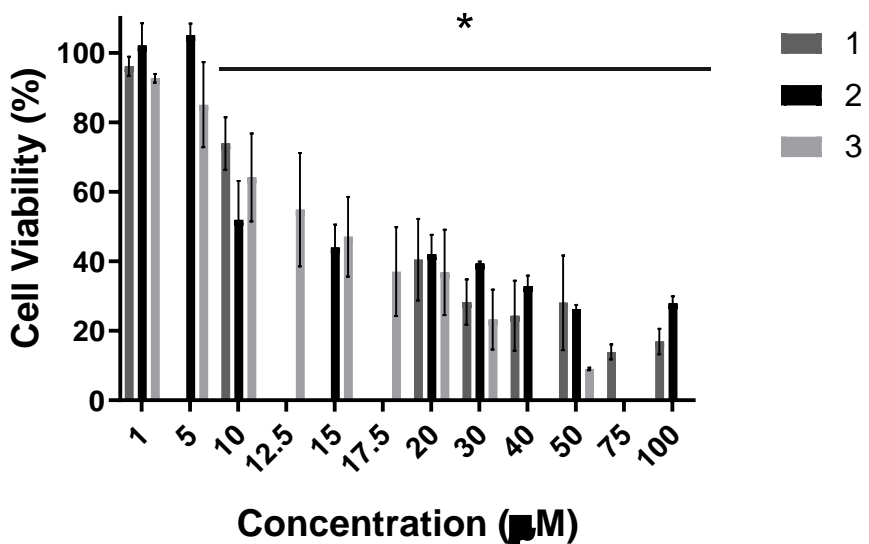


Figure S13. Antiproliferative effect of complexes 1-3 in normal dermal fibroblasts, after 48 h. evaluated by the MTS method. Cell viabilities were normalized to DMSO 0.1% (v/v) (vehicle control). The results presented are mean \pm standard deviation of three independent assays. Asterisk indicates a p-values inferior to 0.05

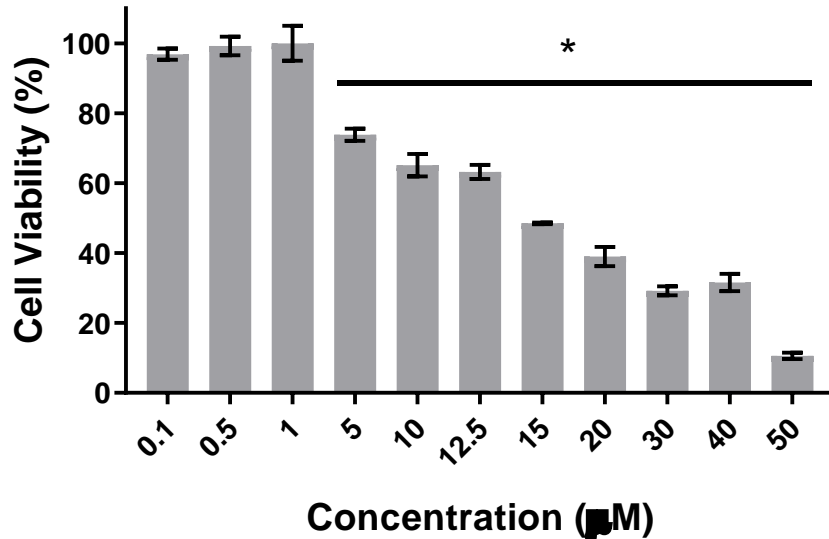


Figure S14. Cell viability of HCT116 cells exposed for 48 h to increasing concentrations of cisplatin. IC_{50} value found is $15.6 \pm 5.3 \mu\text{M}$. * $p < 0.05$ relative to control.